

## Growth and Optical Properties of ZnO Films and Quantum Wells

Zhang Baoping<sup>1,3,†</sup>, Kang Junyong<sup>1</sup>, Yu Jinzhong<sup>1,2</sup>, Wang Qiming<sup>1,2</sup>, and Segawa Yusaburo<sup>3</sup>

(1 Department of Physics, Xiamen University, Xiamen 361005, China)

(2 Institute of Semiconductors, Chinese Academy of Sciences, Beijing 100083, China)

(3 RIKEN, Sendai 980-0845, Japan)

**Abstract:** The growth characteristics during metalorganic chemical vapor deposition and optical properties of ZnO films on sapphire ( $\text{Al}_2\text{O}_3$ ) (0001) and (1120) substrates are studied. For the former, the effects of two important growth parameters, i. e. temperature and pressure, are investigated in detail. Due to the large lattice mismatch between the film and the substrate, ZnO nanocrystals are usually obtained. The growth behavior at the film-substrate interface is found to be strongly dependent on the growth temperature, while the growth pressure determines the shape of the nanostructures as they grow. It is difficult to obtain ZnO films that have good quality and a smooth surface simultaneously. Due to the smaller lattice mismatch, the critical thickness of ZnO on the  $\text{Al}_2\text{O}_3$  (1120) surface is found to be much larger than that on the  $\text{Al}_2\text{O}_3$  (0001) surface. ZnO/MgZnO quantum wells with graded well thicknesses are grown on the  $\text{Al}_2\text{O}_3$  (1120) surfaces, and their optical properties are studied. The built-in electric field in the well layer, generated by the piezoelectric effect, is estimated to be  $3 \times 10^5$  V/cm. It is found that growth at low temperatures and low pressures may facilitate the incorporation of acceptor impurities in ZnO.

**Key words:** ZnO; thin films; quantum well; MOCVD; growth temperature; doping

**PACC:** 6855; 7320D; 7865K

**CLC number:** O484.1

**Document code:** A

**Article ID:** 0253-4177(2006)04-0613-10

### 1 Introduction

Zinc oxide (ZnO) has a wurtzite crystal structure, a large exciton binding energy (60meV,) and a large band gap at room temperature (3.37eV). The research on ZnO is retroactive to 1935 when Bunn reported its lattice properties<sup>[1]</sup>. A comprehensive review of ZnO, in which the research history of ZnO was summarized in detail, has recently been given by Üzgü *et al.*<sup>[2]</sup>. Although ZnO has been studied for a long time in the semiconductor field, it gained substantial interests recently since the discovery of exciton-involved lasing action at room temperature<sup>[3]</sup>. The band gap of ZnO at room temperature is similar to that of GaN (3.39eV), indicating its promising application as a semiconductor light-emitting material in the ultra-violet region. To achieve better-crystalline ZnO for facilitating the formation of stable excitons at room temperature, the growth techniques commonly used in the semiconductor industry are adopted. These include RF magnetron sputtering<sup>[4]</sup>, molecular beam

epitaxy (MBE)<sup>[5]</sup>, metalorganic chemical vapor deposition (MOCVD)<sup>[6]</sup>, and pulsed laser deposition (PLD)<sup>[3]</sup>. ZnO quantum well (QW) structures, which are essential for high-performanced light-emitting devices, have also been fabricated<sup>[7-10]</sup>. The remaining difficulty in the realization of p-type doping seems to be overcome due to the realization of homogeneous ZnO pn junctions and the light emission under the injection of electric current<sup>[11,12]</sup>. However, compared with other kinds of semiconductors, including GaN, studies on ZnO-related films and QWs are still not sufficient, especially in the aspects of the growth behavior, optical properties, reproducibility, and high-concentration p-type doping.

In this paper, we report the effects of the growth temperature and pressure on the crystalline and optical properties of ZnO films grown on sapphire ( $\text{Al}_2\text{O}_3$ ) (0001) and (1120) surfaces. For the former, it is found that a higher growth temperature leads to a better film quality but a rough surface, while a lower growth temperature leads to the opposite results. In addition, at relatively higher

† Corresponding author. Email: bzhang@riken.jp

growth temperatures, simply changing the growth pressure allows us to obtain various ZnO nanostructures such as nanorods, nanotubes, and nanowalls. On  $\text{Al}_2\text{O}_3$  (1120) surfaces, the critical thickness of ZnO is about 10 times larger than that on  $\text{Al}_2\text{O}_3$  (0001) surfaces. ZnO/MgZnO QWs are successfully grown on  $\text{Al}_2\text{O}_3$  (1120) surfaces, and their optical properties are studied. It is also found that growth at low temperatures and under low pressures may be necessary to achieve a high concentration of acceptors in ZnO.

## 2 Experiment

The samples were grown using an MOCVD system with a horizontal rectangular stainless (SUS304) chamber. Oxygen gas ( $\text{O}_2$ ), diethyl zinc (DEZn,  $\text{Zn}(\text{C}_2\text{H}_5)_2$ ), and dimethylcyclopentadienyl magnesium ( $\text{MeCp}_2\text{Mg}$ ) were used as precursors, and nitrogen gas ( $\text{N}_2$ , purity 99.9999%) was used as the carrier gas for DEZn and  $\text{MeCp}_2\text{Mg}$ . The details of the chamber configuration were given in Ref. [13]. The used substrates were (0001) and (1120)  $\text{Al}_2\text{O}_3$ . Before being placed into the chamber, the substrates were degreased in an ultrasonic bath of organic solutions. After pumping down the chamber pressure, the flow of  $\text{O}_2$  was started and the chamber pressure was controlled using a conductance valve. The total flows of  $\text{O}_2$  and  $\text{N}_2$  were 30 ~ 40 sccm and 5 ~ 7 sccm, respectively. The temperature of DEZn and  $\text{MeCp}_2\text{Mg}$  were 4 ~ 5 and 172 °C, respectively. No special thermal treatment to the substrate was done before the growth. The surface morphology was examined using a field-emission scanning electron microscope (FE-SEM, JOEL, JSM-6330F). A four-crystal X-ray diffraction (XRD, Philips X'pert) machine was used to measure the crystalline properties. In photoluminescence (PL) measurements, a He-Cd laser (325nm) was used as the excitation source. The emission from the sample was conducted to a spectrometer (Acton SpectraPro-300i) and detected using a charge-coupled device.

## 3 Results and discussion

### 3.1 ZnO films grown on $\text{Al}_2\text{O}_3$ (0001) surfaces

#### 3.1.1 Effect of growth temperature

The most commonly used substrates for growing single crystalline ZnO are  $\text{Al}_2\text{O}_3$  (0001) wafers, i. e.  $c$ -plane  $\text{Al}_2\text{O}_3$ . Both  $\text{Al}_2\text{O}_3$  and ZnO have a hexagonal crystal structure. The lattice constants for  $\text{Al}_2\text{O}_3$  are  $a = 0.475\text{nm}$ ,  $c = 1.299\text{nm}$ , and for ZnO are  $a = 0.325\text{nm}$ ,  $c = 0.5207\text{nm}$ . On an  $\text{Al}_2\text{O}_3$  (0001) surface, the crystalline relationship of  $c$ -sap  $c$ -ZnO is expected and the  $c$ -axes of both ZnO and  $\text{Al}_2\text{O}_3$  are vertical to the growth plane. For bulk ZnO, every Zn atom is bonded with four oxygen atoms to form a tetrahedral coordination as shown in Fig. 1 (a). This is preferable in ZnO growth because it gives rise to the minimum free energy of the system, which is termed self-texture. When the film is grown on a single crystal surface, competition occurs between the force to grow while maintaining the minimum energy at the film-surface interface and the force to grow while maintaining the self-texture. By changing the growth temperature, we can adjust the balance of these two forces and then control the initial growth behavior at the interface<sup>[14]</sup>. We first grow ZnO films at different temperatures with a fixed growth pressure of 8 ~ 1333 Pa. In epitaxial growth of ZnO on  $\text{Al}_2\text{O}_3$ , the interface energy is mainly composed of strain energy caused by the large lattice mismatch between the film and the substrate. Competition between the forces of keeping smaller strain energy, or smaller lattice mismatch, and that of self-texture will occur. Figure 1 (b) shows the (0001) surface of  $\text{Al}_2\text{O}_3$  and a possible configuration of adsorbed zinc atoms. Here, zinc atoms are located at the lattice sites of the next coming aluminum atoms in the case of  $\text{Al}_2\text{O}_3$  homoepitaxy. In this case, a tetrahedral unit is easily formed by supplying another oxygen atom above a zinc atom. Therefore, this coordination is preferable for both  $\text{Al}_2\text{O}_3$  and ZnO. The unit cell in this case has the same in-plane orientation as that of  $\text{Al}_2\text{O}_3$ , i. e.  $a$ -ZnO  $a$ -sap. This relationship is obtained when the growth temperature is as low as 200 °C<sup>[14]</sup>. ZnO films grown by this mode also have the same lattice constant as that of  $\text{Al}_2\text{O}_3$ , resulting in a very large lattice mismatch (+31.5%, tensile) to ZnO. These results indicate that, at low growth temperatures, the force of self-texture is dominant over that of keeping a smaller lattice mismatch because the diffusion of atoms on the surface is suppressed. On the other hand, when the growth temperature is

higher than 300 ,the kinetic energy of the zinc atoms becomes high enough to diffuse on the substrate surface. These effects cause the zinc atoms to select sites that have a smaller lattice mismatch, and the force of keeping a smaller strain is largely enhanced. One possibility is that the zinc atoms will take the same sites as those of oxygen atoms as shown in Fig. 1 (c). In this case ,a zinc atom is bonded to one oxygen atom in  $\text{Al}_2\text{O}_3$ ,and a tetrahedral coordination of ZnO can be formed by supplying three other oxygen atoms. The oxygen lattice of  $\text{Al}_2\text{O}_3$  has a lattice constant of 0. 275nm ,and the lattice mismatch to ZnO is - 18. 3 % (compressive) ,which is much smaller than the mismatch, 31. 5 % ,obtained in Fig. 1 (b). In Fig. 1 (c) ,the unit cell of ZnO is twisted  $30^\circ$  with respect to that of  $\text{Al}_2\text{O}_3$ . This growth model has been mostly observed in experimental works reported to date.

The ZnO surface morphology exhibits strong dependence on the growth temperature<sup>[14]</sup>. In both cases of Figs. 1 (b) and (c) ,the lattice mismatch is too large to obtain a thick film with a flat surface because of the strain relaxation. The critical thickness for two-dimensional (2D) layer-by-layer growth of ZnO on an  $\text{Al}_2\text{O}_3$  (0001) surface was demonstrated to be only 4. 5nm<sup>[4]</sup>. Therefore , three-dimensional (3D) growth is easily obtained. At higher growth temperatures or in the case of Fig. 1 (c) ,we obtained rough surfaces. An example of such a rough surface is shown in Fig. 1 (e). At lower growth temperatures or in the case of Fig. 1 (b) ,however ,smooth surfaces were obtained as shown by the SEM image in Fig. 1 (d). This may be due to different mechanisms of strain relaxation compared with the growth at higher temperatures. Even though the surface of Fig. 1 (d) was relatively smooth ,XRD measurements revealed a worse crystalline quality caused by the large lattice mismatch between the film and the substrate<sup>[14]</sup>. The effect of the growth temperature can be summarized as follows. A higher growth temperature will enhance the diffusion of absorbed atoms on the surface ,making these atoms find positions that can keep the system at a lower energy. As a result , ZnO films grown at a higher temperature are expected to have better quality. However ,due to the 3D growth mode and the enhanced diffusion of atoms , a rough surface morphology usually occurs. On the contrary ,ZnO films grown at a lower temperature

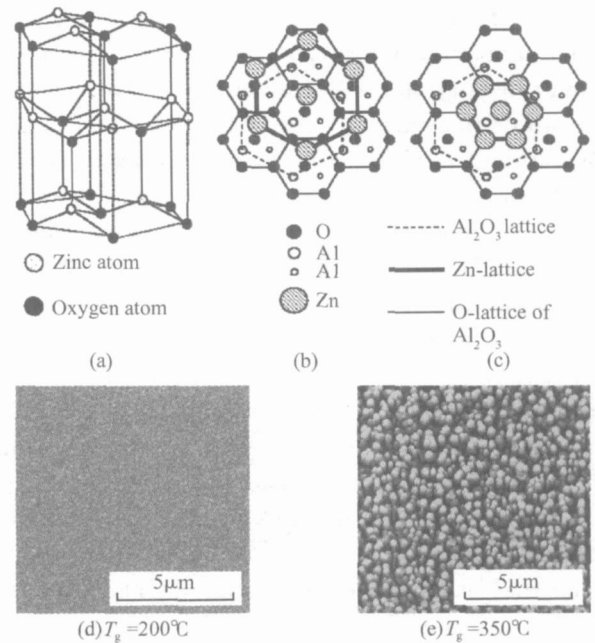


Fig.1 (a) Unit cell of ZnO Each Zn atom is bonded to three oxygen atoms to form a tetrahedral structure ; (b) Possible atomic alignment of Zn on an  $\text{Al}_2\text{O}_3$  (0001) surface at low temperatures where the force of keeping the tetrahedral structure is large. The crystal-line orientation of the ZnO unit cell is the same as that of  $\text{Al}_2\text{O}_3$  ; (c) Possible atomic alignment of Zn on an  $\text{Al}_2\text{O}_3$  (0001) surface at high temperatures where the force of keeping smaller lattice mismatch is large. The ZnO unit cell is twisted for  $30^\circ$  in the growth plane with respect to that of  $\text{Al}_2\text{O}_3$  ; (d) SEM image of a smooth ZnO surface grown at a low growth temperature ( $T_g$ ) ; (e) SEM image of a rough ZnO surface grown at a high growth temperature

have bad quality but a smooth surface. These results were also confirmed by Park *et al.*<sup>[15]</sup>. The conflict between the film quality and the surface morphology makes it very difficult to get films directly on  $\text{Al}_2\text{O}_3$  (0001) surfaces with both a smooth surface and good quality. Nevertheless , the good quality of the films grown at higher growth temperatures allowed us to observe the emission due to bi-exci-tons<sup>[16,17]</sup>. We also studied the optical non-linearity of those ZnO films. The films with bad crystalline quality exhibited the largest second order and third order nonlinear susceptibility ,indicating that the lattice distortion plays an important role<sup>[18,19]</sup>.

PL spectra measured at 4. 2 K from ZnO films

grown at different temperatures are shown in Fig. 2. Each spectrum is normalized by its maximum intensity and is shifted vertically for clarity. For all of the spectra, there are no emission in the visible light region that are usually caused by impurities or defects. The peak at 3.37eV observed for all samples is due to donor-bound exciton emissions ( $D^0X$ ). The emission peak at 3.32eV, which has an intensity comparable to that of the  $D^0X$  exciton, is attributed to emission of donor-acceptor-pairs (DAP) with an acceptor binding energy of 107meV<sup>[16]</sup>. The corresponding acceptor may come from spontaneous nitrogen doping from the carrier gas. The broad emission peak at 3.23eV is attributed to a DAP transition with different kinds of impurities<sup>[20]</sup>. It should be emphasized that acceptor-related emissions at 3.32 and 3.23eV are not observed from the film grown at 500 . This indicates that a higher acceptor concentration may be obtained by growing the film at lower temperatures. In ZnO films grown by pulsed laser deposition, lowering the growth temperature has been demonstrated to be a critical technique to get a higher acceptor concentration<sup>[11,21]</sup>. This approach may also work for MOCVD growth as demonstrated by the PL spectra of Fig. 2.

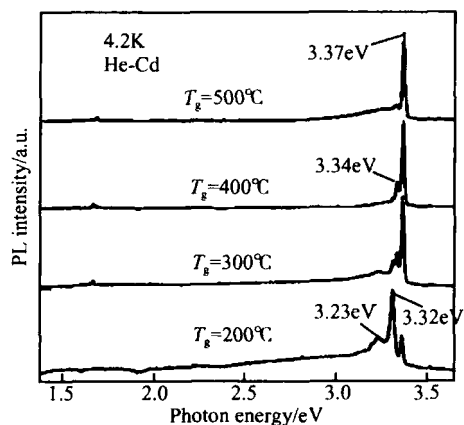


Fig. 2 Low-temperature PL spectra of ZnO films grown at different growth temperatures ( $T_g$ ) on  $Al_2O_3$  (0001) surfaces. The growth pressure is 800Pa for all of the films. Stronger donor-acceptor-pair (DAP) emissions are observed from the films grown at lower temperatures.

### 3.1.2 Effect of growth pressure

The growth pressure in MOCVD is another important factor determining the growth characteristics. We studied the crystalline and optical properties of ZnO films grown under pressures from 8

to 1333Pa and at a fixed growth temperature<sup>[22]</sup>. When the growth temperature is low, for example 200 , both the surface morphology and the optical properties of ZnO films show weak dependence on the growth pressure. However, when the growth temperature is over 300 where the adsorbed atoms are expected to diffuse more, the surface morphology is strongly dependent on the growth pressure, leading to different ZnO nanocrystals such as nanorods, nanotubes, and nanowalls, as shown in Fig. 3. The different shapes of the nanocrystals are believed to be correlated with the total surface energy, and a lower pressure favors a larger surface-to-volume ratio. At a given temperature, when a crystal with a limited volume is formed from the vapor phase, the equilibrium condition requires

$$- P_v \quad ( / V_c)$$

where  $P_v$  is the variation of vapor pressure,  $\gamma$  is the total surface energy which is proportional to the total surface area  $S$ , and  $V_c$  is the volume of the crystal phase. This equation indicates that when the vapor pressure is decreased, the total surface-to-volume ratio ( $S/V_c$ ) must increase. This qualitatively explains the tendency of the nanostructure shapes observed in this study.

Our results show that different nanostructures can be obtained by simply adjusting the growth pressure. Although nanocrystals with different shapes were obtained, the growth behavior at the initial stage was found to be independent of the growth pressure. What we found is that the 3D growth mode is true regardless of the pressure. We believe that this is determined by the film-substrate interface nature. In other words, the large lattice mismatch and the high growth temperature support the 3D growth mode, which does not depend on the growth pressure. However, after a certain growth and when the interface effect becomes weak, the pressure then plays an important role and the structures with different shapes may be expected. The initial nucleation is generally dependent on both the growth condition (surface temperature, reactor pressure, etc.) and the film-substrate lattice mismatch. In our study, the main factors affecting the growth mode are the reactor pressure and the lattice mismatch since the substrate temperature is fixed. In case of ZnO growing on an  $Al_2O_3$  (0001) surface, the lattice mismatch is very large ( $\sim 18\%$ ) and the effect of lattice mismatch is

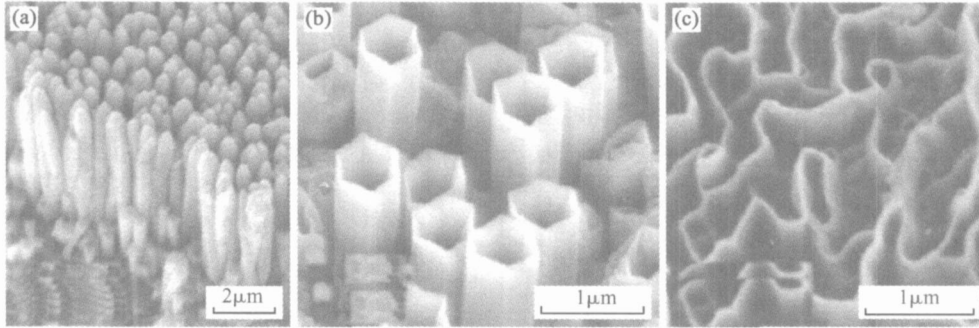


Fig. 3 SEM images of ZnO nanostructures formed at higher growth temperatures (350 ~ 475 °C) under different growth pressures (a) Nanorods ,800Pa ;(b) Nanotubes ,40Pa ;(c) Nanowalls ,8Pa

dominant. Therefore ,clusters at the initial stage of growth are formed. As the growth continues ,the island size increases and the lattice mismatch is relaxed by the formation of defects. After relaxation , the effect of lattice mismatch is weakened and the pressure becomes the dominant factor determining the growth characteristics. In our experiments , when the film thickness is larger than 1μm ,we can constantly obtain nanorods , nanotubes , or nanowalls by simply selecting the reactor pressure.

Figure 4 shows the low-temperature PL spectra of ZnO films grown under different pressures at 400 °C. The peak at 3.366eV is common to all

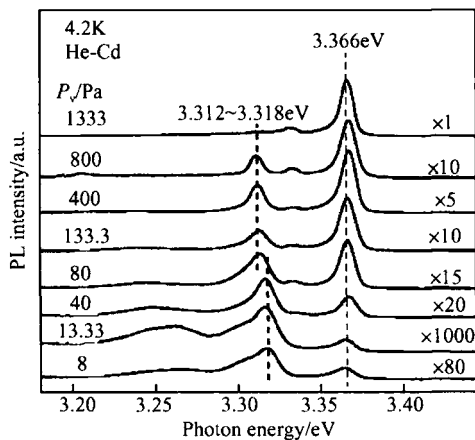


Fig. 4 Low-temperature PL spectra of ZnO films grown under different growth pressures ( $P_v$ ) on  $Al_2O_3$  (0001) surfaces. The growth temperature was 400 °C for all of the films. Large DAP-to- $D^0X$  intensity ratios were observed from films grown under lower pressures.

nanostructures (or all values of  $P_v$ ) and is attributed to  $D^0X$ . The peak located at 3.312 ~ 3.318eV is due to DAP. A general trend is that the DAP-to-

$D^0X$  intensity ratio becomes larger with a decrease in  $P_v$ . This indicates that growth at a lower pressure by MOCVD may enhance the incorporation of acceptors in ZnO. Spontaneous doping of nitrogen , which is known to act as an acceptor ,might have taken place in these structures. Together with the PL results obtained at different growth temperatures shown in Fig. 2 , we may conclude that the growth at low temperatures and low pressures facilitates the incorporation of acceptor impurities.

The overall growth behavior of ZnO is summarized in Fig. 5. ZnO films can be obtained at lower growth temperatures (200 ~ 250 °C) in the throughout pressure range studied. At growth tem-

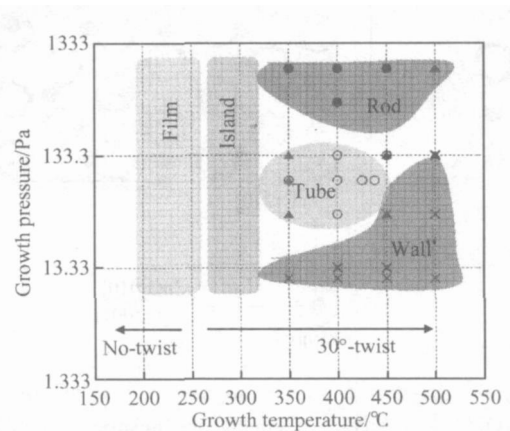


Fig. 5 Summary of ZnO film and nanostructure types grown on  $Al_2O_3$  (0001) surfaces as functions of growth temperature and growth pressure

peratures around 300 °C ,the formation of islands or clusters becomes dominant. With further increase in the growth temperature ,various kinds of nanostructures are expected. Nanorods are obtained under higher pressures (higher than 267Pa) and at

temperatures of 350 ~ 500 . Nanowalls can be easily obtained under lower pressures (less than 26.7 Pa) and in the whole temperature range we studied. Nanotubes can be obtained under pressures of 26.7 ~ 133 Pa and at temperatures of 350 ~ 450 .

### 3.2 Critical thickness of ZnO films on an Al<sub>2</sub>O<sub>3</sub> (1120) surface

ZnO films grown on Al<sub>2</sub>O<sub>3</sub> (1120) surfaces have been demonstrated to exhibit better crystalline quality, although the top surface is the same as that on Al<sub>2</sub>O<sub>3</sub> (0001). The better quality is due to the smaller lattice mismatch and the achievement of single-domain growth as compared with Al<sub>2</sub>O<sub>3</sub> (0001) surfaces<sup>[23]</sup>. As shown in Fig. 6, the epitaxial relationship has been demonstrated to be ZnO (0001) || Al<sub>2</sub>O<sub>3</sub> (1120) and ZnO [010] || Al<sub>2</sub>O<sub>3</sub> [001]. The lattice mismatch along the ZnO [010] direction is less than 0.08% when considering higher order matching ( $4a_{\text{ZnO}} : c_{\text{Al}_2\text{O}_3}$ ). On the other hand, in the ZnO [210] direction, which is perpendicular to both ZnO [010] and ZnO [001], the mismatch is about 2.4% according to the configuration of Fig. 6 ( $\sqrt{3}a_{\text{ZnO}} : 2O_{\text{Al}_2\text{O}_3}$  lattice in Al<sub>2</sub>O<sub>3</sub>). From Figs. 1 (b) or (c), it can be determined that  $O_{\text{Al}_2\text{O}_3} = a_{\text{Al}_2\text{O}_3} / \sqrt{3} = 0.2748 \text{ nm}$ .

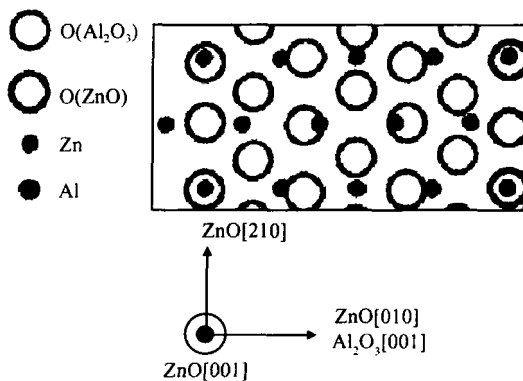


Fig. 6 Suggested atomic alignment of ZnO on an Al<sub>2</sub>O<sub>3</sub> (1120) surface. The lattice mismatch is much smaller compared with that on an Al<sub>2</sub>O<sub>3</sub> (0001) surface.

The critical thickness of ZnO on an Al<sub>2</sub>O<sub>3</sub> (0001) surface has been shown to be 4.5 nm<sup>[4]</sup>. We found that the critical thickness of ZnO on an Al<sub>2</sub>O<sub>3</sub> (1120) surface is much larger due to the small lattice mismatch compared with the case on an Al<sub>2</sub>O<sub>3</sub> (0001) surface<sup>[24]</sup>. The rocking curves of

ZnO (0002) planes are shown in Fig. 7 for films with different thicknesses grown on Al<sub>2</sub>O<sub>3</sub> (1120) surfaces. When the film thickness is no more than 56 nm, only one sharp peak with a full-width at half-maximum (FWHM) value of  $\Delta\omega = 0.005^\circ$  (18) was observed. This value is less than that of

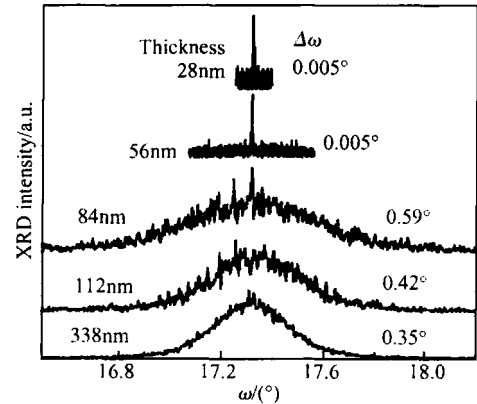


Fig. 7 XRD rocking curves of the ZnO (0002) plane for films of different thicknesses grown on Al<sub>2</sub>O<sub>3</sub> (1120) surfaces. The critical thickness for keeping 2D growth is estimated to be about 56 nm, which is much larger than on an Al<sub>2</sub>O<sub>3</sub> (0001) surface (4.5 nm).

ZnO/Al<sub>2</sub>O<sub>3</sub> (0001) prepared by sputtering (0.019), similar to those (12 ~ 14.4) of ZnO/Al<sub>2</sub>O<sub>3</sub> (0001) grown by MBE and better than that (39) of ZnO films grown on lattice-matched ScAlMgO<sub>4</sub> surfaces. The small  $\Delta\omega$  value obtained from thin films in this study demonstrates a small magnitude of mosaicity and an excellent order along the growth direction of these films. In other words, the films are well aligned, with the *c*-axis strictly parallel to the surface normal within the entire film. This can be taken as an indicator of 2D growth. With a further increase in film thickness, a broad peak appears and, when the film thickness is 84 nm, the latter dominates the rocking curve. The broad peak is centered at the same position as the narrow one, forming a superimposed shape. The superimposed shape of the rocking curve observed in the regime of medium film thickness indicates the coexistence of 2D and 3D layers. For thick films (larger than 112 nm), only the broad peak was observed. Compared with the results obtained for the thin films, the large  $\Delta\omega$  values for the thick films reflect the poorer alignment of the films, which can be attributed to the result of 3D growth. Our results suggest the following growth model: when the thickness is no more than 56 nm, ZnO follows a

2D layer-by-layer growth. However, a 3D growth mode occurs when the film thickness is larger than 112nm. The transition from 2D growth to 3D growth takes place in the thickness range of 56 ~ 112nm. The critical thickness within which the 2D growth of ZnO is realized on an Al<sub>2</sub>O<sub>3</sub> (1120) surface is thus estimated to be 56nm. This is much larger than the value of 4.5nm obtained on an Al<sub>2</sub>O<sub>3</sub> (0001) surface, probably due to the small lattice mismatch in the former.

### 3.3 ZnO/MgZnO QWs on Al<sub>2</sub>O<sub>3</sub> (1120) surfaces

QWs are necessary for the realization of high-performance optoelectronic devices. There have been only a few reports on ZnO-related QWs, and some special substrates have been used. For instance, ZnO/MgZnO multiple QWs have been grown on lattice-matched ScAlMgO<sub>4</sub> surfaces by PLD<sup>[7]</sup>. ZnO/MgZnO single QWs have been grown on GaN surfaces by MOCVD<sup>[8]</sup>. The lattice mismatch between ZnO and GaN is about 2%, which is much smaller than that of commonly used Al<sub>2</sub>O<sub>3</sub> substrates. The disadvantages of such approaches are due to limited supply of ScAlMgO<sub>4</sub> substrates, expensive GaN substrates, and low productivity of the PLD method. Recently, ZnO/MgZnO QWs have been directly grown on Al<sub>2</sub>O<sub>3</sub> (0001) surfaces by radical-source MBE<sup>[10]</sup>. We fabricated ZnO/MgZnO QWs on Al<sub>2</sub>O<sub>3</sub> (1120) surfaces by MOCVD, and we could observe the energy shift caused by the quantum confinement effect, a nearly perfect two-dimensional confinement, and confinement-enhanced exciton recombination<sup>[9]</sup>. Here, we report the results obtained thereafter.

As discussed above, the critical thickness of ZnO on an Al<sub>2</sub>O<sub>3</sub> (1120) surface is much larger than on an Al<sub>2</sub>O<sub>3</sub> (0001) surface. This means that it is easier to obtain ZnO films with smooth surfaces, which is especially important in the preparation of high quality QWs. We developed two approaches to growing ZnO/MgZnO QWs on Al<sub>2</sub>O<sub>3</sub> (1120) surfaces. An MgZnO buffer layer was adopted in both. The buffer layer was grown at 425 °C for about 50nm, followed by an annealing at 800 °C for 10h in an electric furnace. QWs were formed by growing a three-layer MgZnO/ZnO/MgZnO sandwich structure, where MgZnO layers work as barrier and ZnO as well. In the first approach, the MgZnO barriers were grown at low temperatures (~

200 °C) and the ZnO well was grown at 500 °C. After growth, annealing at 700 ~ 900 °C for 2h in the furnace was performed. We have reported some results from the QWs by this approach<sup>[9]</sup>. The fabrication process of the first approach is, however, somewhat complicated. In the second approach, the MgZnO barriers were grown at 425 °C and the ZnO well at 475 °C, and no further thermal treatment was done after growth. From such QWs, besides what was observed from the QWs grown by the first approach, we could further observe the piezoelectric field induced localization. The second approach was found to be a rather simple and reproducible method of growing ZnO/MgZnO QWs.

The sample structure is shown in Fig. 8 in which the layer thickness was dependent on the sample position. By moving the laser spot on the sample surface, we could measure the QW emission at different well widths. Although the barrier

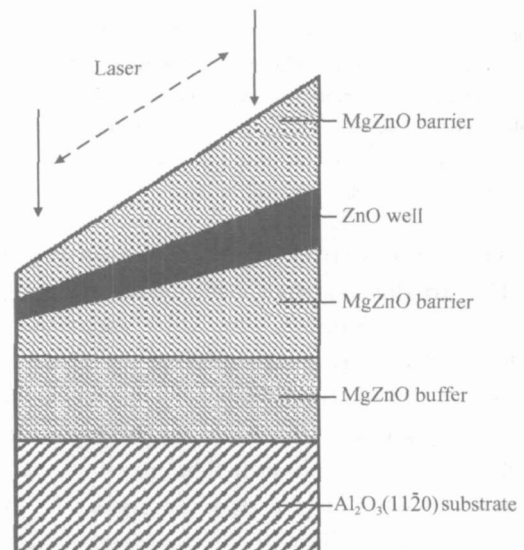


Fig. 8 Illustration of the structure of ZnO/MgZnO QWs. Two different approaches were adopted to fabricate such QWs. The layer thickness was designed to change gradually. The Mg composition is 0.1 in both buffer and barrier layers.

thickness was also position-dependent, it was still much larger than the well thickness, and no quantum confinement effect was expected. In other words, the emission from the barrier was position-independent. Figure 9 (a) shows the position dependence of the PL spectra measured at a sample temperature of 4.2 K. As expected, the emission of

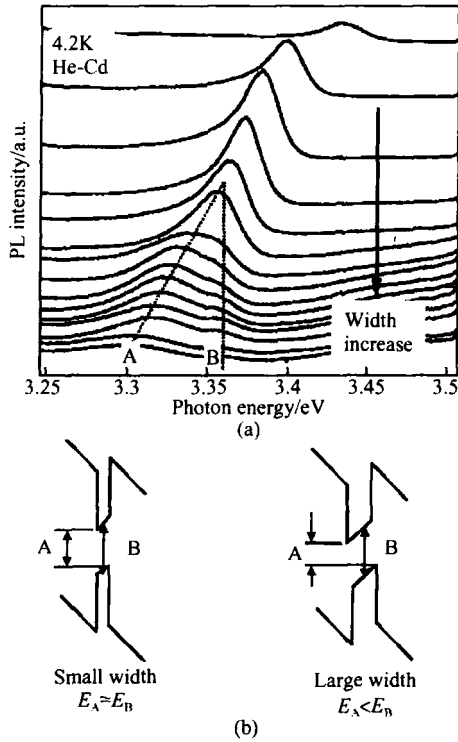


Fig. 9 (a) Low-temperature PL spectra of ZnO/Mg-ZnO QWs measured at different positions of the sample; (b) Illustration of band alignment with a built-in electric field. The emission energies of A and B are almost the same for the small well widths. Their difference becomes larger with the increase of well width.

ZnO QWs shows strong dependence on the position. Due to the quantum confinement effect, the emission peak exhibits a blue shift when the well width is decreased. At relatively larger well widths, an interesting feature appears: a small peak emerges at about 3.36eV on the higher energy side of the QW emission. This peak is position-independent whereas the strong emission from the QW shows a red shift with the increase of the well width. This phenomenon is direct evidence of the built-in electric field generated mainly by piezoelectric effect as shown in Fig. 9 (b). When the well width is large and the quantum confinement effect is negligible, the electric field causes band inclination, and electrons and holes are separately localized at different locations in the well layer. In this case, emissions are possible due to the recombination from both the separately localized electrons and holes (denoted as A) and the band edge of ZnO bulk (denoted as B), and the energy relationship of  $E_A < E_B$  is satisfied. On the other hand, when the well thickness is small enough, the separation of localized electrons and holes becomes small and we have  $E_A \approx E_B$ . In this case, the emission is mainly due to recombination from the quantized energy levels. This phenomenon has been observed in InGaN/GaN and ZnO/MgZnO QWs<sup>[25,26]</sup>. However, previous studies could not observe the effect with a small Mg content, such as 0.1. Moreover, the observation of the present work is much more understandable due to the continuous variation of the well width.

The presence of the electric field inside the well layer is further demonstrated by investigating the dependence of the emission spectra on the excitation power. Figure 10 shows the results in which the excitation power was varied by a few orders of magnitude. The emission peak due to localized electrons and holes was found to exhibit a blue shift with the increase in excitation power. It can be understood as the result of the screen effect of the built-in electric field caused by the excitation-induced carriers. Namely, the electric field causes separation of electrons and holes. Simultaneously, another electric field, which is in the opposite direction to the built-in electric field, is created due to the occurrence of net charged carriers on the two sides of the well layer. When the concentration of electrons and holes are high, as caused by high excitations, the latter electric field gains its strength and finally can compensate the built-in electric field. These effects lead to the blue shift of the emission due to recombination of localized carriers.

The emission peak due to localized electrons and holes was found to exhibit a blue shift with the increase in excitation power. It can be understood as the result of the screen effect of the built-in electric field caused by the excitation-induced carriers. Namely, the electric field causes separation of electrons and holes. Simultaneously, another electric field, which is in the opposite direction to the built-in electric field, is created due to the occurrence of net charged carriers on the two sides of the well layer. When the concentration of electrons and holes are high, as caused by high excitations, the latter electric field gains its strength and finally can compensate the built-in electric field. These effects lead to the blue shift of the emission due to recombination of localized carriers.

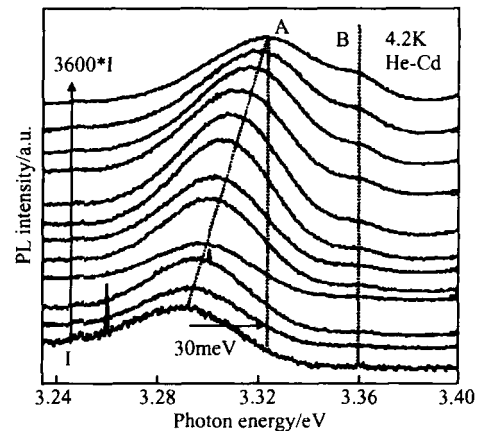


Fig. 10 Excitation power dependence of emission due to recombination of localized electrons and holes induced by the built-in electric field. The blue shift with increase in excitation power is due to the carrier-induced screening of the built-in electric field.

Figure 11 shows the emission energy as a

function of well width obtained at low temperatures. Compared with the free exciton emission from ZnO bulk at 3.376eV, the low-temperature emission energy from the QW can be much lower, e.g., about 16 and 66meV lower for the width-independent and width-dependent ones, respectively. As discussed above, the width-independent one is from ZnO in the thick well. Therefore, we tentatively attribute the 16meV difference to the band gap variation caused by strain. On the other hand, the width-dependent one is due to the recombination of separately-localized electrons and holes. From the slope of the dotted line, the internal electric field is estimated to be  $3 \times 10^5$  V/cm. This value is on the same order as observed in InGaN/ GaN QWs<sup>[25]</sup>.

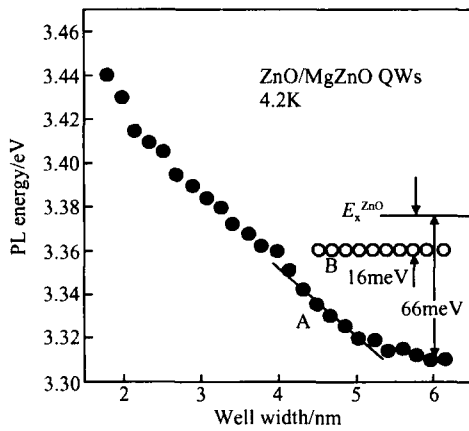


Fig. 11 PL energy versus well width. When the well width is over 4nm, two emissions are observed due to ZnO band edge (denoted as B) and the localized carriers (denoted as A). A built-in electric field of about  $3 \times 10^5$  V/cm is obtained from the slope of the solid line.

## 4 Conclusion

The growth characteristics in MOCVD and optical properties of ZnO films on Al<sub>2</sub>O<sub>3</sub> (0001) and (1120) substrates are studied. For the former, 3D growth is usually expected. The atomic alignment at the film-substrate interface and the crystalline orientation are found to be strongly dependent on growth temperature, while the growth pressure determines the shape of the nanostructures as they are grown. Proper control of growth temperature and pressure allows us to obtain films, rods, tubes, and walls. However, it is difficult to obtain smooth morphology and good quality simultaneously. The critical thickness of ZnO on Al<sub>2</sub>O<sub>3</sub> (112

0) surfaces is more than 10 times larger than that on Al<sub>2</sub>O<sub>3</sub> (0001) surfaces. ZnO/ MgZnO QWs with graded well thicknesses are grown on Al<sub>2</sub>O<sub>3</sub> (1120) surfaces with a simple and reproducible approach. From such QWs, the emission due to the recombination of localized electrons and holes is observed. The built-in electric field in the well is estimated to be  $3 \times 10^5$  V/cm with a Mg composition of 0.1. From the PL spectra, it is apparent that growth at low temperatures and low pressures facilitates the incorporation of acceptor impurities in ZnO.

**Acknowledgement** Part of the work was done in the Photodynamics Research Center, the Frontier Research System of RIKEN. The authors would like to show their sincere acknowledgement to Dr. N. T. Binh, Mr. K. Wakatsuki, Prof. C. Y. Liu and Prof. N. Usami for their fruitful support.

## References

- [ 1 ] Bunn C W. The lattice dimensions of zinc oxide. Proc Phys Soc, 1935, 47 :836
- [ 2 ] Özgür Ü, Alivov Y I, Liu C, et al. A comprehensive review of ZnO materials and devices. J Appl Phys, 2005, 98 :041301
- [ 3 ] Tang Z K, Wong G K L, Yu P, et al. Room temperature ultraviolet laser emission from self-assembled ZnO microcrystallite thin films. Appl Phys Lett, 1998, 72 :3270
- [ 4 ] Part S I, Cho T S, Doh S J, et al. Structural evolution of ZnO/ sapphire (001) heteroepitaxy studied by real time synchrotron X-ray scattering. Appl Phys Lett, 2000, 77 :349
- [ 5 ] Chen Y, Bagnall D M, Koh H J, et al. Plasma assisted molecular beam epitaxy of ZnO on c-plane sapphire: growth and characterization. J Appl Phys, 1998, 84 :3912
- [ 6 ] Ryu Y R, Shu S, Budai J D, et al. Optical and structural properties of ZnO films deposited on GaAs by pulsed laser deposition. J Appl Phys, 2000, 88 :201
- [ 7 ] Makino T, Chia C H, Tuan N T, et al. Room temperature luminescence of excitons in ZnO/ (Mg, Zn) O multiple quantum wells on lattice-matched substrates. Appl Phys Lett, 2000, 77 :975
- [ 8 ] Gruber T, Kirchner C, Kling R, et al. ZnMgO epilayers and ZnO-ZnMgO quantum wells for optoelectronic applications in the blue and UV spectral region. Appl Phys Lett, 2004, 84 :5359
- [ 9 ] Zhang B P, Binh N T, Wakatsuki K, et al. Growth of ZnO/ MgZnO quantum wells on sapphire substrates and observation of the two-dimensional confinement effect. Appl Phys Lett, 2005, 86 :032105
- [ 10 ] Sadofev S, Blumstengel S, Cui J, et al. Growth of high-quality ZnMgO epilayers and ZnO/ ZnMgO quantum well structures by radical-source molecular-beam epitaxy on sapphire. Appl Phys Lett, 2005, 87 :091903
- [ 11 ] Tsukazaki A, Ohtomo A, Onuma T, et al. Repeated temperature modulation epitaxy for p-type doping and light-emitting diode based on ZnO. Nature Mater, 2005, 4 :42

- [12] Jang S, Chen J J, Kang B S, et al. Formation of p-n homojunctions in  $\text{nr-ZnO}$  bulk single crystals by diffusion from a  $\text{Zn}_3\text{P}_2$  source. *Appl Phys Lett*, 2005, 87:222113
- [13] Zhang B P, Wakatsuki K, Binh N T, et al. Low-temperature growth of ZnO nanostructure networks. *J Appl Phys*, 2004, 96:340
- [14] Zhang B P, Wakatsuki K, Binh N T, et al. Effects of growth temperature on the characteristics of ZnO epitaxial films deposited by metalorganic chemical vapor deposition. *Thin Solid Films*, 2004, 449:12
- [15] Park J Y, Lee D J, Yun Y S, et al. Temperature-induced morphological changes of ZnO grown by metalorganic chemical vapor deposition. *J Cryst Growth*, 2005, 276:158
- [16] Zhang B P, Binh N T, Wakatsuki K, et al. Synthesis and optical properties of single crystal ZnO nanorods. *Nanotechnology*, 2004, 15:S382
- [17] Jen F Y, Lu Y C, Chen C Y, et al. Ultrafast biexciton dynamics in a ZnO thin film. *Appl Phys Lett*, 2005, 87:072103
- [18] Liu C Y, Zhang B P, Binh N T, et al. Second harmonic generation in ZnO thin films fabricated by metalorganic chemical vapor deposition. *Opt Commun*, 2004, 237:65
- [19] Liu C Y, Zhang B P, Binh N T, et al. Third-harmonic generation from ZnO films deposited by MOCVD. *Appl Phys B*, 2004, 79:83
- [20] Ryu Y R, Zhu S, Look D C, et al. Synthesis of p-type ZnO films. *J Cryst Growth*, 2000, 216:330
- [21] Tamura K, Ohtomo A, Saikusa K, et al. Epitaxial growth of ZnO films on lattice-matched  $\text{ScAlMgO}_4$  (0001) substrates. *J Cryst Growth*, 2000, 214/215:59
- [22] Zhang B P, Binh N T, Wakatsuki K, et al. Pressure-dependent ZnO nanocrystal growth in a chemical vapor deposition process. *J Phys Chem B*, 2004, 108:10899
- [23] Fons P, Iwata K, Yamada A, et al. Uniaxial locked epitaxy of ZnO on the a face of sapphire. *Appl Phys Lett*, 2000, 77:1801
- [24] Binh N T, Zhang B P, Liu C Y, et al. Structural and optical properties of ZnO epitaxial films grown on  $\text{Al}_2\text{O}_3$  (1120) substrates by metalorganic chemical vapor deposition. *Jpn J Appl Phys*, 2004, 43:4110
- [25] Chichibu S F, Abare A C, Minsky M S, et al. Effective band gap inhomogeneity and piezoelectric field in  $\text{InGaN}/\text{GaN}$  multi-quantum well structures. *Appl Phys Lett*, 1998, 73:2006
- [26] Makino T, Ohtomo A, Chia C H, et al. Internal electric field effect on luminescence properties of  $\text{ZnO}/(\text{Mg}, \text{Zn})\text{O}$  quantum wells. *Physica E*, 2004, 21:671

## ZnO 薄膜和量子阱的生长及光学特性

张保平<sup>1,3,†</sup> 康俊勇<sup>1</sup> 余金中<sup>1,2</sup> 王启明<sup>1,2</sup> 濑川勇三郎<sup>3</sup>

(1 厦门大学物理系, 厦门 361005)

(2 中国科学院半导体研究所, 北京 100083)

(3 独立行政法人 理化学研究所, 仙台 980-0845, 日本)

**摘要:** 研究了用 MOCVD 法在蓝宝石 ( $\text{Al}_2\text{O}_3$ ) (0001) 和 (1120) 衬底上制备 ZnO 薄膜时的生长特性. 详细研究了采用  $\text{Al}_2\text{O}_3$  (0001) 衬底时生长温度与压力的影响. 由于存在比较大的晶格失配, 一般容易得到 ZnO 纳米结晶, 不容易获得既平坦且质量又好的 ZnO 薄膜. 生长温度对薄膜-衬底界面的生长模式有很大的影响; 而生长压力对 ZnO 纳米结晶的形状有决定性作用. 通过适当控制生长温度及压力, 可以得到 ZnO 薄膜或不同形状的纳米结构. 当采用  $\text{Al}_2\text{O}_3$  (1120) 衬底时, 由于晶格失配较小, 能保持平坦层状生长, 临界膜厚远远大于采用  $\text{Al}_2\text{O}_3$  (0001) 衬底的结果. 在  $\text{Al}_2\text{O}_3$  (1120) 衬底上制作了 ZnO/MgZnO 量子阱并研究了其光学特性. 观察到了量子化能级间以及在载流子间的跃迁引起的发光. 由压电效应引起的内建电场约为  $3 \times 10^5 \text{ V/cm}$ . 同时发现采用低温低压生长可以增大 ZnO 中受主杂质浓度, 有利于获得 p 型 ZnO.

**关键词:** 氧化锌; 薄膜; 量子阱; MOCVD; 生长温度; 掺杂

**PACC:** 6855; 7320D; 7865K

**中图分类号:** O484.1

**文献标识码:** A

**文章编号:** 0253-4177(2006)04-0613-10

† 通信作者. Email: bzhang@riken.jp

2005-12-28 收到, 2006-01-19 定稿